

1 An algorithm and codes for fast computations of the opposition effects in a semi-  
2 infinite discrete random medium

3  
4 Victor P. Tishkovets<sup>a,b</sup> and Elena V. Petrova<sup>c</sup>

5  
6 <sup>a</sup> Institute of Radio Astronomy, Kharkiv, Ukraine

7 <sup>b</sup> V.N. Karazin Kharkiv National University, Kharkiv, Ukraine

8 <sup>c</sup> Space Research Institute, Moscow, Russia

9 *emails: [tishkovets@rian.kharkov.ua](mailto:tishkovets@rian.kharkov.ua); [epetrova@iki.rssi.ru](mailto:epetrova@iki.rssi.ru)*

10  
11 We present an algorithm and FORTRAN codes to compute the opposition effects in the  
12 reflection of light from a semi-infinite discrete random medium at normal incidence to the  
13 boundary of the medium. It is assumed that the medium is sparse enough that the waves  
14 propagating between the scatterers are spherical. In this case, the reflection matrix is determined  
15 only by contributions of the incoherent (diffuse) and coherent components. When calculating the  
16 coherent component, the contribution of the doubly scattered radiation to the reflection matrix is  
17 rigorously taken into account, while the contributions of the higher orders are calculated  
18 approximately. To be more specific, the multiply scattered radiation coming to some point of the  
19 medium “from above” is calculated exactly, but the radiation coming “from below”,  
20 approximately. Under this supposition, the solution of the system of integral equations is reduced  
21 to that of the system of linear algebraic equations. The matrix of this system is calculated with  
22 the recurrent relation, which radically speeds up the computations as compared to the direct  
23 procedure. This allows the opposition effect characteristics to be computed rapidly enough so  
24 that the codes may be used in interpretation of the remotely measured intensity and polarization  
25 of light reflected by different media to estimate, at least at a qualitative level, their properties.

26  
27 *Keywords:* multiple scattering; coherent backscattering; opposition effects; discrete random  
28 medium; reflection matrix

29  
30 *Highlights:*

31 A fast algorithm to calculate the opposition effects is presented  
32 FORTRAN codes to compute the opposition effects are described  
33 Errors introduced by the algorithm are concisely considered

## 1 1. INTRODUCTION

2 In the radiation reflected by many discrete media of natural and artificial origin, the so-  
3 called photometric and polarimetric opposition effects are often observed. These phenomena are  
4 usually associated with the weak localization effect, which has been under active experimental  
5 and theoretical examination for the last years (see, e.g., [1–3] and references therein). The  
6 interference nature of this effect suggests that its characteristics essentially depend in the  
7 properties of the scattering medium, which is of key importance for interpretation of remote-  
8 sensing data of different objects. Of particular value is this effect for retrieving the properties of  
9 atmosphereless celestial bodies of the Solar system from the photometric and polarimetric  
10 observational data [4, 5].

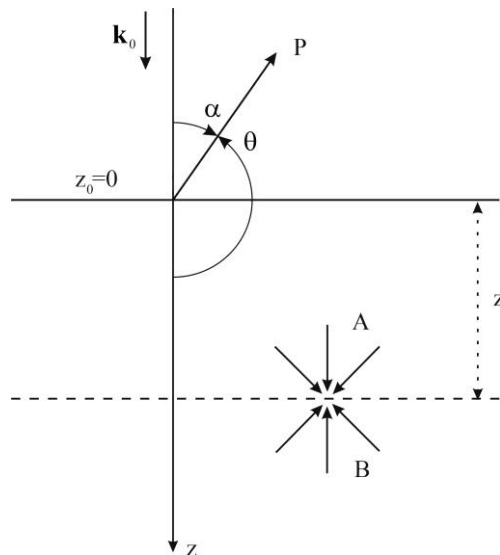
11 In recent years, considerable progress has been made in computations of the weak  
12 localization characteristics for a plane-parallel layer of a medium containing scatterers, the sizes  
13 of which are much larger than the wavelength of the incident radiation. The algorithm described  
14 in [3] makes it possible to calculate the characteristics of this effect (the contribution of cyclical  
15 diagrams into radiation scattered by a medium) with accounting for the near field and the  
16 correlation in particle positions, specifically, under oblique radiation incidence onto the layer.  
17 However, to calculate the characteristics of radiation reflected by random media containing  
18 densely packed scatterers, the sizes of which are of the order of the wavelength, remains an open  
19 problem. The contribution of the other diagrams, particularly, the diagrams responsible for the  
20 mutual shielding or correlation of waves propagating in the medium along neighbor pathways, is  
21 difficult to analyze (see, [2] and references therein).

22 More substantial advances have been made in the description of the weak localization  
23 effect for sparse media, more precisely, in the frames of the model assuming that the waves  
24 propagating between the scatterers in a medium are spherical. In this case the near-field effects  
25 [6] and correlation in particle positions may be ignored, and the scattering characteristics of the  
26 medium are determined only by contributions of the ladder and cyclical diagrams (i.e., the  
27 diffuse and coherent components, respectively) [1–3]. To take into account the dense packing of  
28 particles, at least approximately, it was proposed that randomly oriented clusters should be used  
29 in this model as a volume element of the medium [7]. In this case, all effects connected with the  
30 dense packing of scatterers are automatically accounted for, at least on the scale of clusters. The  
31 comparison of the reflectance characteristics calculated with this model of a semi-infinite  
32 medium to those measured in the laboratory shows that they agree well for some samples [7].  
33 This gives grounds to suppose that this model of a medium can be successfully used to estimate,  
34 at least approximately, the parameters of natural and artificial media investigated remotely.

1 In this paper we describe the efficient algorithm to compute the reflectance characteristics  
 2 of a semi-infinite discrete random medium under normal radiation incidence. This algorithm  
 3 works rapidly, which is of high importance for the remote-sensing data analysis. The single  
 4 scattering matrix of randomly oriented scatterers (in particular, clusters of scatterers) obtained  
 5 from calculations or measurements serve as characteristics of a so-called “elementary (or  
 6 differential) volume element” of the discrete scattering medium, i.e., as input data for the  
 7 procedure.

## 8 2. BASIC RELATIONSHIPS

9 The described algorithm is based on the approximate method of solving the equation for  
 10 weak localization of waves reflected from a semi-infinite discrete random medium under normal  
 11 radiation incidence [8]. To calculate a sum of cyclical diagrams with this method, the radiation  
 12 coming to some point of the medium “from above” is determined exactly, while the radiation  
 13 coming “from below” is taken into account approximately (Fig. 1). Namely, it is assumed that  
 14 the intensity of multiply (more than twice) scattered radiation decreases exponentially with depth  
 15 below the considered point of the medium, while the rate of the decrease can be determined from  
 16 some independent relationship. In this case, the system of integral equations, describing the weak  
 17 localization effect, is reduced to the system of linear algebraic equations. Though all of the basic  
 18 equations were introduced in papers [7, 8], we describe them here with some comments and  
 19 explanations.



20  
 21 Fig. 1. Geometry of scattering by a semi-infinite particulate medium. The incident light  
 22 propagates normally to the boundary of the medium ( $z_0 = 0$ ). The incidence direction is indicated  
 23 by the wave vector  $\mathbf{k}_0$ ,  $\alpha$  and  $\theta$  are the phase and scattering angles, respectively, “P” shows the  
 24 direction of observations, and letters “A” and “B” denote the scattered radiation that comes to  
 25 some point at a depth  $z$  from above and below, respectively.

1

2 The reflection matrix  $\mathbf{S}^{(C)}$ , describing the weak localization effect in the circular-  
3 polarization (CP) representation, is [7, 8]

$$4 \quad S_{pn\nu\mu}^{(C)} = \frac{\pi\eta^2}{k_0^4 \operatorname{Re}(\varepsilon)} \sum_{qq_1LM} (-1)^L \zeta_{LM}^{*(q_1\mu)(qp)} \gamma_{LM}^{(qn)(q_1\nu)}, \quad (1)$$

5 where  $p, n, \mu, \nu, q, q_1 = \pm 1$ , the range of indices  $L, M$  is specified below (see Section3),  $\eta$  is the  
6 particle number density,  $k_0 = 2\pi/\lambda$ ,  $\lambda$  is the wavelength of the incident radiation, the asterisk  
7 denotes complex conjugation,

$$8 \quad \varepsilon = \operatorname{Im}(m_{eff}) \left(1 - \frac{1}{\cos \mathcal{G}}\right) + i(1 + \cos \mathcal{G}) \left(\frac{\operatorname{Re}(m_{eff}) - 1}{\cos \mathcal{G}} + 1\right), \quad (2)$$

9  $m_{eff}$  is the complex effective refractive index of the medium,  $\mathcal{G}$  is the scattering angle, and  
10  $i = \sqrt{-1}$ . For sparse media, it can be assumed that  $m_{eff} = 1 + i\eta C_{ext} / 2k_0$ , where  $C_{ext}$  is the mean  
11 extinction cross-section of scatterers in the medium.

12 The coefficients  $\gamma_{LM}^{(qn)(q_1\nu)}$  are determined from the following system of linear algebraic  
13 equations:

14

$$15 \quad \gamma_{LM}^{(pn)(\mu\nu)} = Q_{LM}^{(pn)(\mu\nu)} + \frac{2\pi\eta}{k_0^3} \sum_{qq_1lm} \chi_l^{(pq)(\mu q_1)} \gamma_{lm}^{(qn)(q_1\nu)} G_{LMlm}^{(N_0)}, \quad (3)$$

16 where

$$17 \quad Q_{LM}^{(pn)(\mu\nu)} = \sum_{lm} \zeta_{lm}^{(pn)(\mu\nu)} \int_0^\pi d_{MN_0}^L(\omega) d_{mN_0}^l(\omega) I_N(c, f) \sin \omega d\omega, \quad (4)$$

$$18 \quad G_{LMlm}^{(N_0)} = \int_0^\pi \left[ I_N(c, f) d_{MN_0}^L(\omega) d_{mN_0}^l(\omega) + (-1)^{L+l+M+m} I_N(c, g) d_{M, -N_0}^L(\omega) d_{m, -N_0}^l(\omega) \right] \sin \omega d\omega. \quad (5)$$

19 Here,  $N = |M - m|$ ,  $d$  with indices are the Wigner  $d$ -functions [9],  $N_0 = \mu - p$ ,

$$20 \quad I_N(c, x) = i^{-N} \frac{c^N}{\sqrt{c^2 + x^2} \left(x + \sqrt{c^2 + x^2}\right)^N}, \quad (6)$$

$$21 \quad c = \sin \mathcal{G} \sin \omega, \quad (7)$$

$$22 \quad f = 2 \operatorname{Im}(m_{eff}) + |\cos \omega| \operatorname{Im}(m_{eff}) \left(1 - \frac{1}{\cos \mathcal{G}}\right) + \quad (8)$$

$$+ i \cos \omega (1 + \cos \mathcal{G}) \left(\frac{\operatorname{Re}(m_{eff}) - 1}{\cos \mathcal{G}} + 1\right),$$

$$23 \quad g = 2 \operatorname{Im}(m_{eff}) (1 + \sigma |\cos \omega|). \quad (9)$$

1 By  $\chi$  with indices, we denote the coefficients of the Wigner  $d$ -function expansions of the  
 2 single scattering matrix averaged over orientations and properties of scatterers in the CP-  
 3 representation (the scattering matrix for a volume element in the medium). The analogous  
 4 coefficients in the linear-polarization (LP) representation, though in the basis of the generalized  
 5 spherical function closely related to the Wigner functions, are widely used in the radiative  
 6 transfer theory to calculate the diffuse component of the reflection matrix for different media  
 7 [10]. Their explicit form for spherical and randomly oriented irregular scatterers and the  
 8 formulas to convert from the CP-basis to the LP-basis and back can be found in a paper [13].

9 The quantities  $\zeta$  with indices are coefficients that have not appeared in the scattering  
 10 theory before. For spherical scatterers, the formulas required for calculating these coefficients  
 11 are given in papers [2, 7, 11], where their physical content is considered in detail. For arbitrary  
 12 scatterers, a calculation technique to obtain the coefficients  $\zeta$  is still lacking. It was shown in  
 13 papers [2, 11] that, for spherical particles and at  $\mathcal{G} \approx \pi$ , the following approximation is valid

$$14 \quad \zeta_{lm}^{(pn)(\mu\nu)} \approx \delta_{m,v-n} \chi_l^{(pn)(\mu\nu)}, \quad (10)$$

15 where  $\delta_{m,v-n}$  is the Kronecker delta. This approximation made it possible to generalize the weak-  
 16 localization equation obtained for a medium of spherical particles to the case of arbitrary  
 17 scatterers, for which the coefficients  $\chi$  can be calculated. Specifically, this is true for a medium  
 18 of the scatterers, the scattering matrix of which is measured in laboratory, if the examination is  
 19 thorough enough that the coefficients  $\chi$  can be calculated. In the following, we assume that  
 20 approximation (10) is obeyed.

21 As has been already mentioned, when deriving the above equations, we suppose that the  
 22 radiation coming from below and scattered more than twice decreases exponentially with  
 23 growing the depth  $z$  in the layer. We assume that this dependence takes the form  
 24  $\exp(-2\sigma z \text{Im}(m_{\text{eff}}))$ , where the coefficient  $\sigma$  characterizes the rate of the decrease of the  
 25 radiation intensity with depth. This coefficient is determined from the relationship that connects  
 26 the reflection matrix elements of the incoherent component with those for weak localization in  
 27 the exactly backscattering direction ( $\mathcal{G} = \pi$ ). These relationships for the diagonal matrix  
 28 elements are given in papers [10] and [11] in the LP and CP representations, respectively. For a  
 29 semi-infinite medium, an analogous approach to deriving the contribution of radiation coming  
 30 from below is proposed in a paper [3]; however, a more complicated nonlinear dependence of  
 31 the exponent on the depth  $z$  is introduced in that study. The fast algorithm proposed here for  
 32 computing the characteristics of the weak localization effect can be applied to both the linear and  
 33 nonlinear dependences of the exponent on  $z$ .

Let us point to the following property of Eqs. (1)–(5). In papers [3, 12], the weak localization equations are written in such a way that they contain the single-scattering contribution, which is then removed. In Eqs. (1)–(5) above, the single-scattering contribution is already absent. Coefficients (4) correspond to the double scattering, and they are calculated in a rigorous manner, so that the approximation mentioned at the beginning of this section is used only for the higher orders of the scattered radiation coming from below.

In actual practice, the reflection matrix in the LP representation  $\mathbf{R}$  is used

$$\mathbf{R} = \mathbf{R}^{(L)} + \mathbf{R}^{(C)}. \quad (11)$$

Here,  $\mathbf{R}^{(L)}$  is the reflection matrix of the diffuse component, while the elements of the reflection matrix of the coherent component in the LP basis  $\mathbf{R}^{(C)}$  take the form

$$\begin{aligned} R_{11}^{(C)} &= U \sum_{pn} S_{pnpn}^{(C)}, & R_{21}^{(C)} = R_{12}^{(C)} &= -U \sum_{pn} S_{pn-pn}^{(C)}, & R_{22}^{(C)} &= U \sum_{pn} S_{pn-p-n}^{(C)}, \\ R_{33}^{(C)} &= U \sum_{pn} S_{pn-p-n}^{(C)} i^{p-n}, & R_{44}^{(C)} &= U \sum_{pn} S_{pnpn}^{(C)} i^{p-n}, & R_{34}^{(C)} &= -R_{43}^{(C)} = iU \sum_{pn} S_{pn-p-n}^{(C)} i^{p-n}, \end{aligned} \quad (12)$$

where  $U = -\pi / 2k_0^2 \cos \mathcal{G}$  and  $n, p = \pm 1$ .

### 3. A FAST ALGORITHM TO COMPUTE THE COHERENT REFLECTION MATRIX

The computing speed in solving system (3) is mainly determined by the computing speed for matrix (5). The dimension of the matrix depends on the sizes of scatterers and the scattering angle. The highest value of the index  $L$  depends on the sizes of scatterers and is determined by the required accuracy of calculations of the coefficients  $\chi$ . For example, for spherical particles, the highest value of the index  $L$  is equal to the double value of the highest summation index  $l_m$  in the Mie formulas (see, e.g., [13]). In general,  $-L \leq M \leq L$ . Because of this, the dimension of matrix (5) is  $[2l_m(2l_m + 1)] \times [2l_m(2l_m + 1)]$ ; consequently, for the medium composed of scatterers larger than the wavelength in size, the matrix dimension may be very large. For example, for the medium composed of spherical scatterers with the size parameter  $x_0 = 5$  ( $x_0 = k_0 a$ , where  $a$  is the scatterer radius), for which the maximal summation index can be determined as  $l_m = x_0 + 4.05x_0^{1/3} + 8$  [13], the dimension of matrix (5) is  $1640 \times 1640$ . When approximation (10) is used, the matrix dimension falls dramatically to roughly  $200 \times 200$  at  $\mathcal{G} = \pi$  or to somewhat larger dimensions at smaller scattering angles.

The computations of so large matrices can be made much faster with recurrent relation (A.4) given in the Appendix. To use it, it is convenient to rewrite the integral in Eq. (4) as follows:

$$1 \quad \int_0^{\frac{\pi}{2}} \left[ I_N(c, f) d_{MN_0}^L(\omega) d_{mN_0}^l(\omega) + (-1)^{L+l+M+m} I_N(c, f^*) d_{M-N_0}^L(\omega) d_{m-N_0}^l(\omega) \right] \sin \omega d\omega. \quad (13)$$

2 As is seen from Eqs. (4), (5), and (13), calculations of the matrix of system (5) and  
3 coefficients (4) are reduced to calculations of the integrals such as

$$4 \quad F_{LMN_1}^{lmN_1} = \int_0^{\frac{\pi}{2}} I_N(c, x) d_{MN_1}^L(\omega) d_{mN_1}^l(\omega) \sin \omega d\omega, \quad (14)$$

5 where  $N_1 = \pm N_0$ .

6 Though the recurrent relation (A.4) is applicable directly to integral (14), a more efficient  
7 way is to expand the products of the Wigner functions to a series in the Wigner functions, i.e.,

$$8 \quad F_{LMN_1}^{lmN_1} = (-1)^{m+N_1} \sum_{L_1=|L-l|}^{L+l} C_{LMl-m}^{L_1M_1} C_{LN_1l-N_1}^{L_10} \int_0^{\frac{\pi}{2}} I_{|M_1|}(c, x) d_{M_10}^{L_1}(\omega) \sin \omega d\omega. \quad (15)$$

9 Here the  $C$ 's with indices are the Clebsch–Gordan coefficients [9], and  $M_1 = M - m$ .  
10 Relationship (15) completely corresponds to (A.7) from the Appendix, which formula (A.4) can  
11 be applied to.

12 Since the symmetry relation  $d_{M_0}^L(\omega) = (-1)^M d_{-M_0}^L(\omega)$  [9] is obeyed, the integral in the right  
13 side of Eq. (15) may be calculated only for positive and zero values of  $M_1$ . The reflection matrix  
14 may be computed substantially faster also by using the following symmetry relations [7]:

$$15 \quad F_{LMN_1}^{lmN_1} = F_{lmN_1}^{LMN_1} = (-1)^{M+m} F_{L,-M,-N_1}^{l,-m,-N_1} \quad G_{LMlm}^{(N_0)} = (-1)^{M+m} G_{L,-Ml-m}^{(-N_0)}$$

$$16 \quad Q_{LMlm}^{(pn)(\mu\nu)} = (-1)^{M+m} Q_{L,-Ml-m}^{(-p-n)(-\mu-\nu)} \quad \gamma_{LM}^{(pn)(\mu\nu)} = (-1)^M \gamma_{L-M}^{(-p-n)(-\mu-\nu)}$$

17 Thus, the matrix of system (5) and coefficients (4) may be computed according to the  
18 following algorithm. The arrays of values of the integrals in the right side of Eq. (15) are  
19 calculated for  $x = f$ ,  $x = g$ , and the scattering angle  $\mathcal{G} = \pi$ . With the recurrent formula (A.4)  
20 (see also relationship (A.7) in the Appendix), the integrals of type (15) are calculated; then,  
21 coefficients (4) and matrix (5) are found. System (3) is solved, and the value of  $\sigma$  is determined  
22 with some method chosen. The computational procedure is repeated with the obtained value of  
23  $\sigma$  to find coefficients (4) and matrix (5) and to solve system (3) for the other scattering angles  
24 specified.

#### 25 4. COMPUTATIONAL CODES

26 The described procedure was realized in the software package [14], the codes of which are  
27 written in the Fortran-90 programming language. The coherent component of the reflection

1 matrix  $\mathbf{R}^{(C)}$  is calculated on the base of approximation (10). The coefficient  $\sigma$  is found from the  
 2 equation

$$3 \quad R_{11}^{(C)} = (R_{11}^{(M)} + R_{22}^{(M)} - R_{33}^{(M)} + R_{44}^{(M)})/2, \quad (16)$$

4 which is valid for  $\mathcal{G} = \pi$  [13] and solved with the simple bisection method. Here the matrix  
 5  $\mathbf{R}^{(M)} = \mathbf{R}^{(L)} - \mathbf{R}^{(1)}$ , and  $\mathbf{R}^{(1)}$  corresponds to the single scattering.

6 To solve system (3), the iteration Bi-CGSTAB method [15] is used. The main program  
 7 *opp\_eff.f90* operates in conjunction with the file of input parameters *data\_inp.txt* and other files  
 8 specified there. The *data\_inp.txt* file contains the following data:

9 *Number of integration intervals*: this parameter specifies the number of identical subintervals  $K$ ,  
 10 which the entire integration interval ( $\omega = \pi/2$ ) in integral (15) is divided into. The  
 11 Chebyshev quadrature formula is used for integration in each of the subintervals. As a  
 12 rule,  $K = 6$  is sufficient for calculating the integrals of type (15) with a high accuracy  
 13 even for very large scatterers.

14 *alp0, dalp1, alp1, dalp2, alp2, dalp3, alp3*: these are the boundaries of three predetermined  
 15 intervals for changing the phase angles  $\alpha$  ( $\alpha = \pi - \mathcal{G}$ )---from 0 to  $\alpha_1$ , from  $\alpha_1$  to  $\alpha_2$ ,  
 16 and from  $\alpha_2$  to  $\alpha_3$  (*alp0, alp1, alp2, alp3*); and each of them may have its own step of  
 17 changes in  $\alpha$  ---  $\Delta\alpha_1$ ,  $\Delta\alpha_2$ , and  $\Delta\alpha_3$  (*dalp1, dalp2, dalp3*), respectively.

18 *Relative particle concentration*:  $\xi = \frac{4\pi a_v^3}{3} \eta$ , where  $a_v$  is the radius of the volume-equivalent  
 19 sphere of a scatterer in the medium.

20 *Output file*: the name of the file containing the result of computations of the  $\mathbf{R}^{(C)}$  matrix  
 21 elements.

22 *Input file of the single-scattering matrix expansion coefficients*: the name of the file containing  
 23 the characteristics of a volume elements of the medium. This file should be prepared  
 24 beforehand. Its structure is described below.

25 *Input file of the incoherent reflection matrix*: the name of the file containing the  $\mathbf{R}^{(L)}$  matrix  
 26 elements obtained in calculations of the incoherent component of the reflection matrix.  
 27 As the previous file, it should be prepared beforehand. Its structure is also described  
 28 below.

29 The first line of the *Input file of the single-scattering matrix expansion coefficients* should  
 30 contain the values of the following characteristics of a volume element of the medium: the single  
 31 scattering albedo  $\tilde{\omega} = Q_{sca} / Q_{ext}$  (where  $Q_{sca}$  and  $Q_{ext}$  are the scattering and extinction efficiency  
 32 factors, respectively), the maximal value of the index  $L$ ,  $Q_{sca}$ , the asymmetry parameter



1  $\langle \cos \vartheta \rangle$ , and the equivalent size parameter  $x_v = k_0 a_v$ . The efficiency factors are defined with  
2 respect to the volume-mean radius  $a_v$  of the volume element. The other lines contain the  
3 expansion coefficients of the normalized scattering matrix of the volume element in generalized  
4 spherical functions in the LP basis. The elements should be in the following succession in the  
5 line:  $\alpha_1^s$ ,  $\alpha_2^s + \alpha_3^s$ ,  $\alpha_2^s - \alpha_3^s$ ,  $\alpha_4^s$ ,  $\beta_1^s$ , and  $\beta_2^s$ , where  $\alpha_1^s$ ,  $\alpha_2^s$ ,  $\alpha_3^s$ ,  $\alpha_4^s$ ,  $\beta_1^s$ , and  $\beta_2^s$  are the  
6 expansion coefficients of the scattering matrix elements  $a_{11}(\vartheta)$ ,  $a_{22}(\vartheta)$ ,  $a_{33}(\vartheta)$ ,  $a_{44}(\vartheta)$ ,  $a_{21}(\vartheta)$ ,  
7 and  $a_{34}(\vartheta)$ , respectively; and  $0 \leq s \leq \max(L)$ . In this file, the scattering matrix in the LP  
8 representation is expanded in the basis of the generalized spherical functions, since the latter is  
9 traditional in the theory of light scattering by small particles and widely used in the radiative  
10 transfer theory [10, 13].

11 The  $\mathbf{R}^{(L)}$  matrix elements should be in the *Input file of the incoherent reflection matrix*;  
12 the sequence of the quantities in each of the lines in this file is:  $\vartheta$  ( $90^\circ \leq \vartheta \leq 180^\circ$ ),  $R_{11}^{(L)}$ ,  $R_{12}^{(L)}$ ,  
13  $R_{21}^{(L)}$ ,  $R_{22}^{(L)}$ ,  $R_{33}^{(L)}$ , and  $R_{44}^{(L)}$ . The scattering angle step in calculations of this matrix should be small  
14 enough near the backscattering direction for further interpolating to those specified for the  $\mathbf{R}^{(C)}$   
15 matrix. The last line should contain the matrix elements for  $\vartheta = 180^\circ$ . The values from this line  
16 are used to solve equation (16) and find the coefficient  $\sigma$ . The  $\mathbf{R}^{(L)}$  matrix may be computed  
17 with any code available. For example, the code described in a paper [16] produces the diffuse  
18 matrix elements in the format applicable to the present procedure.

19 To find the reflection matrix  $\mathbf{R}$  (Eq. (11)), the  $\mathbf{R}^{(L)}$  matrix elements are interpolated  
20 according to the phase angle values, which were specified in calculations of the coherent  
21 component  $\mathbf{R}^{(C)}$  in the *data\_inp.txt* file. The obtained elements of the  $\mathbf{R}$  matrix are written to  
22 the file called *REFL\_Output file.txt*. Its first line contains the heading; and  $x_v$ ,  $1/(2k_0 l_{tr})$ ,  $\sigma$ ,  $\xi$ ,  
23 and  $\text{Im}(m_{eff})$  are in the second line. Here,  $l_{tr} = \text{Im}(m_{eff})(1 - \langle \cos \vartheta \rangle)$  is the transport free-path.  
24 The third line contains the diagonal elements of the incoherent matrix  $\mathbf{R}^{(L)}$  taken from the *Input*  
25 *file of the incoherent reflection matrix*, while the same elements, but calculated from the  
26 elements of the coherent matrix  $\mathbf{R}^{(C)}$  with the equations connecting the coherent and incoherent  
27 components at  $\alpha = 0$  ( $\vartheta = \pi$ ), are in the fourth line. Since the latter are determined for the  
28 obtained value of  $\sigma$ , they show how correct the approximation works for these matrix elements  
29 and the specified parameters of the medium. In the fifth line, there are values of the left and right  
30 parts of Eq. (16), respectively, under the obtained  $\sigma$ . The other lines contain the two elements of  
31 the reflection matrix  $\mathbf{R}$  ---  $R_{11}(\alpha)$  and  $R_{21}(\alpha)$  --- and the derived quantities: the normalized first

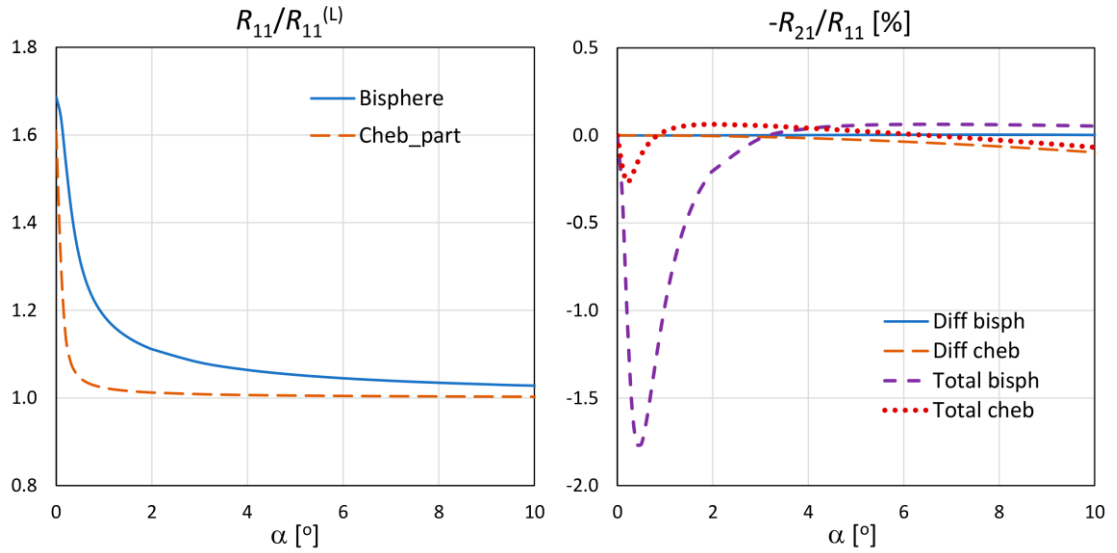
1 element  $R_{11}(\alpha)/R_{11}(0)$ , the linear polarization degree  $-R_{21}(\alpha)/R_{11}(\alpha)\times 100$ , and the  
2 enhancement factor  $R_{11}(\alpha)/R_{11}^{(L)}(\alpha)$ .

### 3 5. APPLICATION EXAMPLES

4 In many applications, for example, when analyzing the remote sensing data, there is a need  
5 to simulate numerically the reflectance characteristics of discrete random media rather rapidly. In  
6 this paper, we propose the algorithm and codes for fast computations of the weak localization  
7 characteristics (the opposition effects). This algorithm uses the approximation developed in a  
8 paper [8] for sparse semi-infinite discrete random medium under the normal radiation incidence  
9 onto the medium boundary. The algorithm is based on introducing the recurrent formula (A.4)  
10 into calculations of the matrix of system (3), which substantially diminishes the processing time  
11 as compared to that of direct computations of the matrix elements. For example, to calculate the  
12 coherent reflection matrix for the medium containing randomly oriented bispheres with a size  
13 parameter of monomers  $x_0 = 2$  and the refractive index  $\tilde{m} = 1.5 + i0.1$ , the use of formula (A.4)  
14 requires the processing time an order of magnitude smaller than the direct computations. For  
15 larger scatterers, the time saving may be much more effective.

16 The results of computations with the described codes are presented in Fig. 2. The  
17 enhancement factor and the linear polarization degree for the above described bispheres and  
18 Chebyshev polydisperse particles are shown versus the phase angle in the backscattering domain.  
19 The parameters of Chebyshev particles are: the effective size parameter corresponding to the  
20 equal-volume sphere  $x_v = 2.5$ , the effective variance of the power-law distribution  $v_{eff} = 0.05$   
21 and  $\tilde{m} = 1.51 + i0.0$ ; their shape is specified by  $r(\vartheta) = r_0(1 - 0.1T_8(\vartheta))$ , where  $r_0$  is the radius of  
22 the unperturbed sphere and  $T_8(\vartheta)$  is the Chebyshev polynomial. The relative particle  
23 concentration  $\xi$  is assumed to be 0.01 for the both media. It is worth noting that, for bispheres,  
24 this value corresponds to the concentration of particles rather than bispheres (see [7]).

25



1  
2 Fig. 2. The enhancement factor (left) and the linear polarization degree (right) for  
3 bispheres and Chebyshev particles (see the text for details) in dependence on the phase angle in  
4 the backscattering domain. The quantities obtained from the total reflection matrix elements and  
5 the diffuse (incoherent) contribution are shown for polarization.

## 6 7 6. CONCLUDING REMARKS

8 Let us analyze the inaccuracy of the proposed method. First, errors may be caused by the  
9 usage of the approximation, where the double-scattering contribution is rigorously accounted for  
10 while the higher-order contributions to the radiation coming from below is calculated under the  
11 assumption of the exponential decrease of the intensity with depth [8]. With increasing the  
12 absorption in the medium, the assumption on the radiation exponentially weakening with depth  
13 becomes closer to the truth and the calculations of the reflection matrix yield more accurate  
14 results. The second source of errors is the use of approximation (10). The weaker the dependence  
15 of the scattering matrix of a volume element on the scattering angle near  $\mathcal{G} = \pi$ , the smaller the  
16 inaccuracy caused by this approximation.

17 Of course, these are only inaccuracies introduced by the approximations assumed when  
18 solving the initial equation [8, 11, 12]. The latter, as the other equations describing the weak  
19 localization effect (see, e.g., [3] and references therein), was itself obtained under some  
20 suppositions. The limits of applicability of these assumptions could be estimated from the  
21 reflectance characteristics of discrete medium samples measured in the laboratory with  
22 completely controlled samples. In particular, this would make it possible to define the limits of  
23 applicability of the far-zone approximation, within which the waves propagating between the  
24 scatterers are assumed to be spherical. Consequently, this would allow us to estimate the highest  
25 concentration of scatterers in the medium appropriate for this approximation. The results of

1 numerical solution of the vector radiative transfer equation were compared to the reflection  
 2 matrix elements of suspensions of submicron latex particles in water measured in the laboratory,  
 3 and it was found that the far-zone approximation can be applied to the media with packing  
 4 densities smaller than  $\sim 5\%$  [17]. This suggests that, for the coherent component of the reflected  
 5 radiation, this approximation is also valid up to the same packing densities of particles.  
 6 Unfortunately, measurements with completely controlled samples are still lacking, which does  
 7 not allow us to determine more precisely the applicability limits of the far-field approximation  
 8 and other assumptions of the described algorithm. However, at a qualitative level, it was  
 9 successfully tested by the laboratory data for some samples [7, 18]. Consequently, the proposed  
 10 algorithm may be used at least to estimate the parameters of the media when interpreting the  
 11 remote sensing data, particularly, the data of ground-based observations of the Solar system  
 12 bodies [18, 19].

### 13 ACKNOWLEDGMENTS

14 The authors are grateful to M. Mishchenko and D. Mackowski for making available the T-  
 15 matrix computational codes ([https://www.giss.nasa.gov/staff/mmishchenko/t\\_matrix.html](https://www.giss.nasa.gov/staff/mmishchenko/t_matrix.html),  
 16 [www.eng.auburn.edu/~dmckwski/scatcodes/](http://www.eng.auburn.edu/~dmckwski/scatcodes/)) and to M. Mishchenko for providing us with the  
 17 code to compute the diffuse component of the reflection matrix, a complete version of which is  
 18 freely accessible on <https://www.giss.nasa.gov/staff/mmishchenko/brf/>. The authors thank the  
 19 reviewers for valuable comments.

### 20 FUNDING

21 The work by V.P. Tishkovets was supported by the Marie Skłodowska-Curie Research  
 22 Innovation and Staff Exchange (RISE) (the GRASP-ACE grant no. 778349).

## 24 APPENDIX. RECURRENT RELATION: DERIVATION AND APPLICATION 25 SCHEME

26 We derive here a recurrent relation, which is used to calculate the matrix elements, and  
 27 describe a scheme of its application.

28 Let us consider the integral

$$29 \quad V_{LMN}^{l+1,mn} = \int f(\omega) d_{MN}^L(\omega) d_{mn}^{l+1}(\omega) \sin \omega d\omega, \quad (A.1)$$

30 where  $f(\omega)$  is an arbitrary integrable function. The following recurrent relation [9] will also be  
 31 used

$$32 \quad \cos \omega d_{mn}^l(\omega) = a_{lmn} d_{mn}^{l+1}(\omega) + c_{lmn} d_{mn}^l(\omega) + b_{lmn} d_{mn}^{l-1}(\omega), \quad (A.2)$$

33 where

$$1 \quad a_{lmn} = \frac{\sqrt{[(l+1)^2 - m^2][(l+1)^2 - n^2]}}{(l+1)(2l+1)}, \quad b_{lmn} = \frac{\sqrt{(l^2 - m^2)(l^2 - n^2)}}{l(2l+1)}, \quad c_{lmn} = \frac{nm}{l(l+1)}. \quad (\text{A.3})$$

2 Let us multiply (A.1) to  $a_{lmn}$  and apply relationship (A.2) to (A.1), namely, sequentially to  
3  $a_{lmn}d_{mn}^{l+1}(\omega)$  and  $\cos \omega d_{MN}^L(\omega)$ . This yields the following recurrent relation for the integral  $V_{LMN}^{lmn}$ :

$$4 \quad a_{lmn}V_{LMN}^{l+1,mn} + (c_{lmn} - c_{LMN})V_{LMN}^{lmn} + b_{lmn}V_{LMN}^{l-1,mn} - a_{LMN}V_{L+1,MN}^{lmn} - b_{LMN}V_{L-1,MN}^{lmn} = 0. \quad (\text{A.4})$$

5 Relationship (A.4) is multipurpose. It can be applied to some functions that are frequent in  
6 the light scattering theory. For example, it can be applied to the product of two Clebsch–Gordan  
7 coefficients. To demonstrate this, we will use the expansion of the product of two Wigner  
8 functions [9]

$$9 \quad d_{MN}^L(\omega)d_{mn}^l(\omega) = \sum_{k=|L-l|}^{L+l} C_{LMlm}^{kM_1} C_{LNln}^{kN_1} d_{M_1N_1}^k(\omega). \quad (\text{A.5})$$

10 Here,  $M_1 = M + m$  and  $N_1 = N + n$ . Let us apply formula (A.2) to the left part of (A.5) in the  
11 same way as in deriving relationship (A.4) above. Expand the obtained products of two Wigner  
12 functions into series of type (A.5) and introduce

$$13 \quad W_{LMN}^{lmn}(k) = C_{LMlm}^{kM_1} C_{LNln}^{kN_1}. \quad (\text{A.6})$$

14 Taking into account the orthogonal property of the Wigner functions [9], we obtain a  
15 recurrent relation analogous to (A.4) for the coefficients  $W_{LMN}^{lmn}(k)$  under fixed  $k$ . By multiplying  
16 relation (A.6) to an arbitrary function  $f_{M_1N_1}^k$ , which is independent of the indices  $L$  and  $l$ , and  
17 summing up the product over all possible  $k$ , we obtain a recurrent formula analogous to (A.4)  
18 for the coefficients  $F_{LMN}^{lmn}$ :

$$19 \quad F_{LMN}^{lmn} = \sum_{k=|L-l|}^{L+l} C_{LMlm}^{kM_1} C_{LNln}^{kN_1} f_{M_1N_1}^k. \quad (\text{A.7})$$

20 In particular, the recurrent relation (A.4) is valid for the coefficients of the translational  
21 addition theorem for spherical vector wave functions (see, e.g., [2, 3, 19, 20])

$$22 \quad H_{LMlm} = \sum_{k=|L-l|}^{L+l} C_{LMl-m}^{kM_1} C_{Lql-q}^{k0_1} z_k(k_0 r) D_{M_10}^k(\varphi, \vartheta, 0). \quad (\text{A.8})$$

23 Here,  $q = \pm 1$ ,  $z_k(k_0 r)$  is the Bessel or Hankel spherical function,  $D_{M_10}^k(\varphi, \vartheta, 0)$  is the Wigner  
24 function [9]. The recurrent relation (A.4) for the coefficients of the translational addition theorem  
25 for spherical vector wave functions was obtained earlier in [20] and used in [21] to calculate the  
26 scattering matrix of aggregates.

27 Relationship (A.4) may be used according to the following procedure. As it appears from  
28 the properties of the Wigner functions [9], the coefficients  $V_{LMN}^{lmn}$  (as well as coefficients

1 (A.6)–(A.8)) are zero for  $L < \max(|M|, |N|)$  or  $l < \max(|m|, |n|)$ . Assume that, in the matrix of  
2 the coefficients  $V_{LMN}^{lmn}$ , the elements of the first nonzero line ( $l = \max(|m|, |n|)$ ) and the last  
3 column ( $L = L_{mzx}$ ) are known. Then the elements of the second line are calculated with formula  
4 (A.4), and all coefficients  $V_{LMN}^{l-1mn} = 0$  for this line. Since the matrix of the coefficients  $V_{LMN}^{lmn}$  is  
5 symmetric relative to the main diagonal, it will suffice to calculate only the elements of the upper  
6 triangular matrix. Analogously, only the elements of the lower triangular matrix of the  
7 coefficients  $V_{LMN}^{lmn}$  may be calculated, if the elements of the first nonzero column of the matrix  
8  $L = \max(|M|, |N|)$  and the last line are precalculated.  
9  
10

## 1 REFERENCES

- 2 [1] Mishchenko MI. Multiple scattering, radiative transfer, and weak localization in discrete  
3 random media: the unified microphysical approach. *Rev Geophys* 2007;46: RG2003.  
4 <https://doi.org/10.1029/2007RG000230>.
- 5 [2] Tishkovets VP, Petrova EV, Mishchenko MI. Scattering of electromagnetic waves by  
6 ensembles of particles and discrete random media. *J Quant Spectrosc Radiat Transfer*  
7 2011;112:2095–127. <https://doi.org/10.1016/j.jqsrt.2011.04.010>.
- 8 [3] Doicu A, Mishchenko MI. Electromagnetic scattering by discrete random media. IV:  
9 Coherent backscattering. *J Quant Spectrosc Radiat Transfer* 2019; 236:106565.  
10 <https://doi.org/10.1016/j.jqsrt.2019.07.008>.
- 11 [4] Polarimetry of stars and planetary systems. Kolokolova L, Hough J, Levasseur-Regourd AC,  
12 editors. Cambridge: Cambridge University Press; 2015.  
13 <https://doi.org/10.1017/CBO9781107358249>.
- 14 [5] Mishchenko MI, Rosenbush VK, Kiselev NN, Lupishko DF, Tishkovets VP, Kaydash VG,  
15 Belskaya IN, Efimov YS, Shakhovskoy NM. Polarimetric remote sensing of Solar System  
16 objects. Kyiv: Akadempriodyka; 2010.
- 17 [6] Tishkovets VP, Petrova EV. Light scattering by densely packed systems of particles: near-  
18 field effects. In: Kokhanovsky AA, editor. Springer series in light scattering reviews. 7.  
19 Radiative transfer and optical properties of atmosphere and underlying surface, Springer;  
20 2012, p. 3–36.
- 21 [7] Tishkovets VP, Petrova EV Coherent backscattering by discrete random media composed of  
22 clusters of spherical particles. *J Quant Spectrosc Radiat Transfer* 2013;127:192–206.  
23 <https://doi.org/10.1016/j.jqsrt.2013.05.017>.
- 24 [8] Tishkovets VP, Mishchenko MI. Approximate calculation of coherent backscattering for  
25 semi-infinite discrete random media. *J Quant Spectrosc Radiat Transfer* 2009;110:139–45.  
26 <https://doi.org/10.1016/j.jqsrt.2008.09.005>.
- 27 [9] Varshalovich DA, Moskalev AN, Khersonskii VK. Quantum theory of angular momentum.  
28 Singapore: World Scientific; 1988.
- 29 [10] Mishchenko MI, Travis LD, Lacis AA. Multiple scattering of light by particles. Radiative  
30 transfer and coherent backscattering. Cambridge: Cambridge University Press; 2006.
- 31 [11] Tishkovets VP, Mishchenko MI. Coherent backscattering of light by a layer of discrete  
32 random medium. *J Quant Spectrosc Radiat Transfer* 2004;86:161–80.  
33 [https://doi.org/10.1016/S0022-4073\(03\)00281-4](https://doi.org/10.1016/S0022-4073(03)00281-4).
- 34 [12] Tishkovets VP. Multiple scattering of light by a layer of discrete random medium:  
35 backscattering. *J Quant Spectrosc Radiat Transfer* 2002;72:123–37.  
36 [https://doi.org/10.1016/S0022-4073\(01\)00059-0](https://doi.org/10.1016/S0022-4073(01)00059-0).
- 37 [13] Mishchenko MI, Travis LD, Lacis AA. Scattering, absorption, and emission of light by  
38 small particles. Cambridge: Cambridge University Press; 2004.
- 39 [14] <http://rian.kharkov.ua/index.php/en/software-en>
- 40 [15] Van der Vorst HA. Bi-CGSTAB: a fast and smoothly converging variant of Bi-CG for the  
41 solution of nonsymmetric linear systems. *SIAM J Sci Stat Comput* 1992;13(2):631–44.  
42 <http://dx.doi.org/10.1137/0913035>.
- 43 [16] Mishchenko MI, Dlugach JM, Chowdhary J, Zakharova NT. Polarized bidirectional  
44 reflectance of optically thick sparse particulate layers: An efficient numerically exact  
45 radiative-transfer solution. *J Quant Spectrosc Radiat Transfer* 2015;156:97–108.  
46 <http://dx.doi.org/10.1016/j.jqsrt.2015.02.003>.
- 47 [17] Mishchenko MI, Goldstein DH, Chowdhary J, and Lompado A. Radiative transfer theory  
48 verified by controlled laboratory experiments. *Opt Lett* 2013;38:3522–5.

- 1 [18] Tishkovets VP, Petrova EV. Reflectance model for densely packed media: estimates of the  
2 surface properties of the high-albedo satellites of Saturn. *Sol Syst Res* 2017; 51:277–93.  
3 <https://doi.org/10.1134/S0038094617040062>.
- 4 [19] Petrova EV, Tishkovets VP, Nelson RM, Boryta MD. Prospects for estimating the  
5 properties of a loose surface from the phase profiles of polarization and intensity of the  
6 scattered light. *Sol Syst Res* 2019;53:172–80.  
7 <https://doi.org/10.1134/S0038094619020059>.
- 8 [20] Chew WC, Wang YM. Efficient ways to compute the vector addition theorem. *Journal of*  
9 *Electromagnetic Waves and Applications* 1993;7:651–65.  
10 <https://doi.org/10.1163/156939393X00787>.
- 11 [21] Mackowski DW, Mishchenko MI. A multiple sphere T-matrix FORTRAN code for use on  
12 parallel computer clusters. *J Quant Spectrosc Radiat Transfer* 2011;112:2182–92.  
13 <https://doi.org/10.1016/j.jqsrt.2011.02.019>.

14

## 15 FIGURE CAPTIONS

16 Fig. 1. Geometry of scattering by a semi-infinite particulate medium. The incident light  
17 propagates normally to the boundary of the medium ( $z_0 = 0$ ). The incidence direction is indicated  
18 by the wave vector  $\mathbf{k}_0$ ,  $\alpha$  and  $\vartheta$  are the phase and scattering angles, respectively, “P” shows the  
19 direction of observations, and letters “A” and “B” denote the scattered radiation that comes to  
20 some point at a depth  $z$  from above and below, respectively.

21 Fig. 2. The enhancement factor (left) and the linear polarization degree (right) for  
22 bispheres and Chebyshev particles (see the text for details) in dependence on the phase angle in  
23 the backscattering domain. The quantities obtained from the total reflection matrix elements and  
24 the diffuse (incoherent) contribution are shown for polarization.

25